Interfacial and structural properties of sputtered HfO 2 layers

G. Aygun and I. Yildiz

Articles you may be interested in

In-situ spectroscopic ellipsometry and structural study of HfO2 thin films deposited by radio frequency magnetron sputtering
J. Appl. Phys. **116**, 083517 (2014); 10.1063/1.4893708

Ultrathin TiSiN overcoat protection layer for magnetic media
J. Vac. Sci. Technol. A **29**, 051502 (2011); 10.1116/1.3607423

Temperature-dependent structural stability and optical properties of ultrathin Hf–Al–O films grown by facing-target reactive sputtering
J. Appl. Phys. **102**, 094103 (2007); 10.1063/1.2802994

Interfacial chemical structure of Hf O 2∕Si film fabricated by sputtering
Appl. Phys. Lett. **89**, 142907 (2006); 10.1063/1.2358841

Spectroscopic characterization of high k dielectrics: Applications to interface electronic structure and stability against chemical phase separation
J. Vac. Sci. Technol. A **22**, 1301 (2004); 10.1116/1.1755714

Interfacial and structural properties of sputtered HfO$_2$ layers

G. Aygun[1,a)] and I. Yildiz[2,3]
[1]*Department of Physics, Izmir Institute of Technology, Urla, TR-35430 İzmir, Turkey*
[2]*Department of Physics, Middle East Technical University, TR-06531 Ankara, Turkey*
[3]*Central Laboratory, Middle East Technical University, TR-06531 Ankara, Turkey*

Magnetron sputtered HfO$_2$ layers formed on a heated Si substrate were studied by spectroscopic ellipsometer (SE), x-ray diffraction (XRD), Fourier transform infrared (FTIR), and x-ray photoelectron spectroscopy (XPS) depth profiling techniques. The results show that the formation of a SiO$_x$ suboxide layer at the HfO$_2$/Si interface is unavoidable. The HfO$_2$ thickness and suboxide formation are highly affected by the growth parameters such as sputtering power, O$_2$/Ar gas ratio during sputtering, sputtering time, and substrate temperature. XRD spectra show that the deposited film has (111) monoclinic phase of HfO$_2$, which is also supported by FTIR spectra. The atomic concentration and chemical environment of Si, Hf, and O have been measured as a function of depth starting from the surface of the sample by XPS technique. It shows that HfO$_2$ layers of a few nanometers are formed at the top surface. Below this thin layer, Si–Si bonds are detected just before the Si suboxide layer, and then the Si substrate is reached during the depth profiling by XPS. It is clearly understood that the highly reactive sputtered Hf atoms consume some of the oxygen atoms from the underlying SiO$_2$ to form HfO$_2$, leaving Si–Si bonds behind. © *2009 American Institute of Physics*. [DOI: 10.1063/1.3153953]

I. INTRODUCTION

In order to overcome the scaling limit of conventional Si-based insulators due to high tunneling currents and reliability concerns, high-permittivity (high-κ) materials, such as single metal oxides and their silicates as well as ferroelectrics, are being developed as alternative dielectrics. Among the high-κ materials, such as TiO$_2$, Y$_2$O$_3$, Ta$_2$O$_5$, ZrO$_2$, and HfO$_2$ metal oxides, having high-κ values at around 25 and being thermodynamically stable when grown on Si, HfO$_2$ is considered to be the most promising candidate to replace SiO$_2$.[1] Important film properties such as the dielectric constant and refractive index of the grown film depend on the growth parameters as well as the initial thin film constitution. Moreover, the interface properties of the film play a crucial role in the electrical properties of the devices. It is, then, of interest to analyze this type of a film as a function of depth by chemical-structural diagnostic techniques such as x-ray photoelectron spectroscopy (XPS).

Even though Gibbs free energy predicts a stable layer for the formation of HfO$_2$ on Si,[2,3] an interfacial layer formation between HfO$_2$ and Si has been shown by various experimental work.[2,4,5] In order to minimize the effects of this unavoidable interfacial layer, different methods have been proposed by various groups. Tan *et al.*[6] predeposited about 1 nm Hf metal layer before depositing HfO$_2$. They showed that after a 30 s deposition of the Hf metal on a Si substrate, the equivalent thickness of the silicate layer was reduced from ~3.5 nm to a value of about 1.9 nm. They concluded that Hf radicals reduced SiO$_2$ to metallic Si to form HfO$_2$ and partly HfSi$_x$.

Similarly, Hayashi *et al.*[4] deposited 0, 1.3, 2.6, and 3.9 nm thick Hf metals on Si, followed by HfO$_2$ growth on this thin Hf metal layer. They showed from cross-section transmission electron microscopy images of oxidized HfO$_2$ layers with a thin Hf metal on top of a Si substrate that the thickness of the interfacial layer decreased with an increment in Hf metal layer thickness, i.e., a 2.8 nm interfacial layer with 1.6 nm hafnium oxide without any thin Hf metal while a 0.5 nm interfacial layer with 7.0 nm hafnium oxide for 3.9 nm Hf metal on a Si substrate. They concluded that a thin deposited Hf metal interacted with the introduced oxygen inside the oxidation chamber, and therefore, the introduced thin Hf metal had a role to inhibit oxygen diffusion into the Si substrate. They summarized their results that oxygen species react primarily with the Hf metal covering the Si surface to result in HfO$_2$, and therefore, Si oxidation was suppressed.

In order to get rid of the unintentional growth of this interfacial layer, Kirsch *et al.*[2] tried the method of nitridation of a Si substrate before the oxidization process. They first etched the native oxide on *p*-Si(100) wafers by dipping in a 1% hydrofluoric acid solution for 1 min and then nitrided it at 700 °C in 1 atm NH$_3$ for 30 s. Afterwards, Hf oxidation and rapid thermal annealing (RTA) densification processes were realized. XPS results' comparisons corresponding to O 1*s*, Si 2*p* and N 1*s* regions for the HfO$_2$/Si interface of un-nitrided and nitrided samples after HfO$_2$ deposition and densification processes showed that although nonstoichiometric hafnium silicate (HfSi$_x$O$_y$) forms at both types of substrates, i.e., HfO$_2$/Si and HfO$_2$/SiN$_x$, silicate feature appeared at 532.1 eV had 15% larger intensity on the un-nitrided substrate than that of the nitrided substrate. Additionally, Si 2*p* spectra had 102.8 eV feature corresponding to HfSi$_x$O$_y$ for both samples, nevertheless, it is larger by a factor of 2 for the un-nitrided substrate. Their results, there-

a)Electronic mail: gulnuraygun@iyte.edu.tr.

fore, showed that SiN_x minimizes the interfacial $HfSi_xO_y$ formation by limiting the available Si amount for the possible interaction with the HfO_2 layer.

A number of compatible methods have been developed to fabricate high-κ materials such as thermal oxidation,[4] a variety of chemical vapor deposition techniques,[7] ion beam deposition,[8] atomic layer deposition,[9,10] pulsed laser deposition,[11] laser oxidation,[12] remote plasma oxidation,[13] and dc and rf sputtering.[4,5] Since each method has some advantages and disadvantages, it is not yet clear which one would be the best choice for device applications.

Because the native oxide of Si, namely, SiO_2, is a perfect insulator than any other material, this layer, in this work, was kept on the p-Si(100) substrate and after chemical cleaning, a HfO_2 layer was grown by dc reactive sputtering of a Hf target on native oxide. This paper presents a depth profile analysis of a reactively grown HfO_2 thin film by a dc sputtering technique on a p-Si(100) substrate having native oxide. The interface structure is studied in a more detailed manner to understand the kinetics of different material formations taking place at the interface region.

II. EXPERIMENTAL PROCEDURE

HfO_2 thin film was grown on a Si substrate by a reactive dc magnetron sputtering technique in high vacuum. A p-type Si(100) substrate with resistivity of $7-17$ Ω cm was chemically cleaned in boiling trichloroethylene and acetone together with an ultrasonic bath of ultrapure water. After the cleaning process, it was dried with pure N_2 gas and mounted onto the substrate holder, which has a 7.4 cm distance to the target of the magnetosputtering deposition chamber vacuumed with a turbomolecular pump. In spite of the high purity of the Hf target, 3 min presputtering with Ar gas flow was done to prevent a possible surface contamination of the target. A 12 SCCM (SCCM denotes cubic centimeter per minute at STP) O_2 and 30 SCCM Ar ($O_2/Ar=0.4$) gas mixture and a 2 in. diameter and 0.250 in. thick 99.9% pure hafnium target were used. The base pressure of the sputtering chamber was below 2×10^{-6} Torr, while the working pressure during the sputtering was 0.44×10^{-3} Torr. Prior to, as well as during deposition, the substrate was heated by a halogen lamp and the substrate's temperature was adjusted by a temperature controller. As can be seen in Fig. 1, the thin film deposition rate can be controlled by both the dc source and the gas flow level of reactive O_2 and the Ar gas mixture. The substrate temperature and the dc power were kept at 200 °C and 30 W, respectively, for a 5 min sputtering time duration for this growth process.

A Fourier transform infrared (FTIR) spectrometer (Bruker Equinox 55) was used to obtain information on both the chemical composition and the structure of the film. The crystallinity of the film was examined by taking an x-ray diffraction (XRD) pattern (Rigaku Miniflex system equipped with Cu $K\alpha$ radiation of an average wavelength of 1.541 Å). The XRD pattern was analyzed by a computer software and an ICDD (the International Centre for Diffraction Data) database, which includes the diffraction patterns of well known
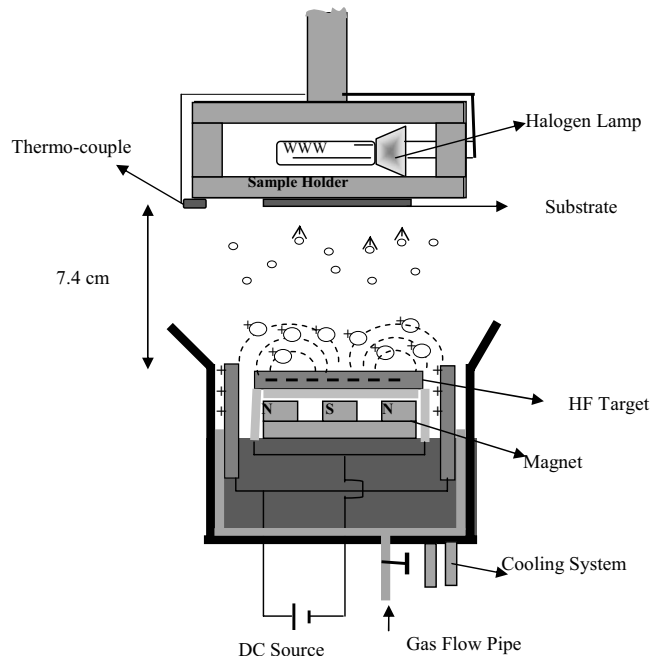

FIG. 1. Cross sectional inside view of the sputtering chamber with sample holder used for dc sputtering method.

structures. The peak matching process was carried out based on the observed peak positions at specific 2θ values and relative intensities of the peaks.

A spectroscopic ellipsometer (SE) measurement of thin HfO_2 film on p-Si(100) was made in the wavelength range of 300–850 nm using Sentech SE-801. The SE measurement at a 70° incident light beam on the sample surface was done in the surrounding of air at room temperature to obtain DELTA (Δ) and PSI (Ψ). SPECTRARAY program was used for the modeling and fitting processes of the SE data, i.e., Δ and ψ, to the measured ones. The outcomes of the modeling and fitting processes were refractive index (n), thickness (d), and transmission and absorption (κ) of the medium.

XPS measurements were done at a vacuum level of 7.5 $\times10^{-10}$ Torr with a SPECS EA200 (Electron Spectroscopy for Chemical Analysis) system equipped with a hemispherical electron analyzer at a takeoff angle of 90°. The excitation source was a monochromatic Al $K\alpha$ line with a power of 490 W. The film surface was sputtered by Ar^+ ions having an energy of 2000 eV with a total of 19 cycles (etched layer numbers) each taking 3 min to obtain the depth profiles with respect to Si, O, Hf, and C atoms. XPS measurements were done with a 96 eV pass energy and a 0.1 eV step size. Binding energies were corrected with respect to an elemental Si $2p$ peak at 99.3 eV for depth layers, while a C $1s$ peak at 284.6 eV was used for the surface. Background correction and peak fit features were performed to the data using CASA XPS software.

III. RESULTS AND DISCUSSION

A. FTIR spectra of dc sputtered HfO_2 films

Figure 2 shows the FTIR spectrum of the Hf-oxide layer grown at 200 °C for 5 min at 30 W of dc sputtering power. The spectra were taken between 400 and 4000 cm^{-1}, but
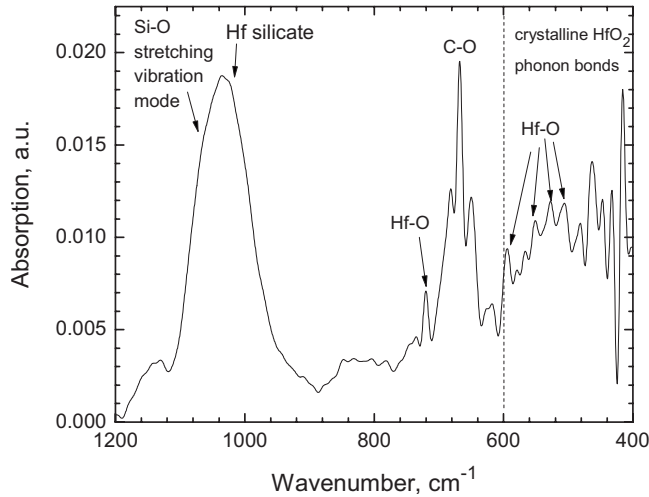
FIG. 2. Absorption spectra obtained from FTIR spectroscopy.

FIG. 3. XRD pattern of the film.

since the low wavenumber region (<1100 cm^{-1}) is more important for the detection of hafnium-oxide-related bonds, only the region of 400–1200 cm^{-1} is presented in the figure. Since OH peaks (around 3300–3400 cm^{-1}) cannot be detected in the spectrum, this region is not shown. The absence of these signals, on the other side, suggests that the film is moisture free. Moreover, no hydrocarbon absorption peaks are detected at around 3000–1600 cm^{-1}, which indicates a negligible organic residue present in the as deposited films.

As can be clearly visualized from the figure, the observed broad and very intense absorption band standing between 950 and 1120 cm^{-1} can be decomposed into two intensive peaks located in the vicinity of 1060 and 1020 cm^{-1} corresponding to the Si–O stretching vibration mode and hafnium silicate (HfSi$_x$O$_y$), respectively.[14] The peak intensity reflects the film thickness so that there is a very thick hafnium silicate layer. However, having a close location but not around the exact position of the natural oxide of SiO$_2$ (1075 cm^{-1}) implies that this interfacial oxide layer is in the form of a suboxide of Si instead of the natural oxide form, i.e., SiO$_x$ with $x < 2$.[7]

The main peaks at around 595, 550, 527, and 506 cm^{-1} are due to the Hf–O chemical bonds, and so is the 720 cm^{-1} one.[15,16] It can be concluded that the presence of sharp HfO$_2$ phonon bonds in the low wavenumber region (600–400 cm^{-1}) is the result of the crystalline structure of the grown film.[9] However, the most intensive features of HfO$_2$ are reported in the 100–500 cm^{-1} region, most of which extend outside of our measurement range (lower than 400 cm^{-1}).[16] Since FTIR measurement was done in air, as a result, the C–O vibration mode is detected at its expected position at around 670 cm^{-1}.[17]

B. XRD structural properties

XRD was performed for 2Θ being in the range of 10–65° at room temperature for HfO$_2$ film grown on p-type Si(100) with natural SiO$_2$ oxide. It is clearly observed that there is a peak at around 28° of 2Θ attributed to the (111) monoclinic phase of HfO$_2$ (Fig. 3).[16,18–20]

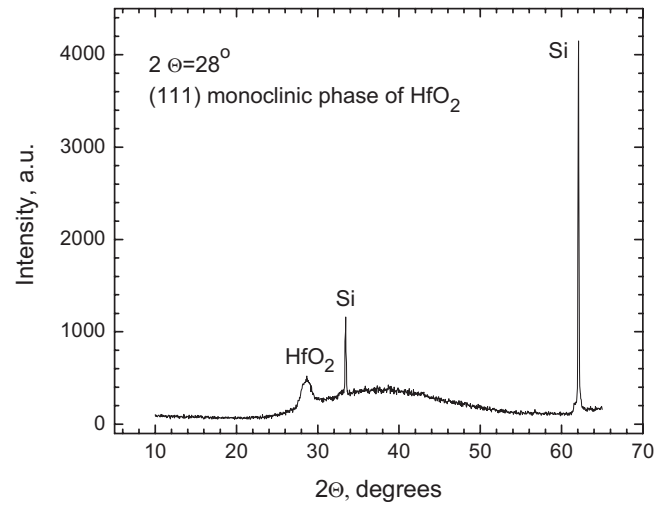Having a low peak intensity and a high full width at half maximum value, it can be inferred that the microcrystalline structure has just started to form. This is supposed to be the result of the film grown at the elevated substrate temperature of 200 °C but would not be the case for the film grown at room temperature. Pereira et al.[18] studied the sputter grown HfO$_2$ thin film's structural analysis using XRD with respect to substrate temperature changes from the room temperature to 200 °C during growth. They also recognized a peak at 2Θ being around 28° when the substrate temperature was increased to 200 °C, even though an amorphous structure was detected at the room temperature growth process. The other two intensive peaks at around 33.3° and 62.1° in Fig. 3 are the signals coming from the Si(100) substrate of thin hafnium-oxide film. This microcrystalline structure of HfO$_2$ film can also be predicted from the sharpness of the phonon spectrum in the 400–600 cm^{-1} region of the FTIR spectrum, as seen in Fig. 2.[9]

C. SE

An ellipsometer works on the basis of the change in polarization state during reflection off of a light from a film surface at an oblique angle of incidence, PHI (Φ). Detailed theoretical calculations for obtaining the equations of an ellipsometer can be easily found in the literature.[21,22] Matching the electric and magnetic fields at the interface between different materials, the complex reflection ratio, RHO (ρ), is obtained as

$$\rho = \tan \Psi e^{i\Delta}, \tag{1}$$

where Ψ, Δ, and ρ are the parameters of the ellipsometer, and there is a relation between the optical and electrical parameters of bulk materials:

$$\varepsilon = \varepsilon_1 + i\varepsilon_2 = \sin^2 \phi \left[1 + \tan^2 \phi \left(\frac{1-\rho}{1+\rho} \right)^2 \right]. \tag{2}$$

After obtaining the Ψ and Δ of the grown film with respect to wavelength in the range of 300–850 nm by means of SE, the sputter grown HfO$_2$ film on the p-Si(100) substrate was modeled as air/HfO$_2$ film/SiO$_2$/c-Si(100) (Fig. 4). The thick-
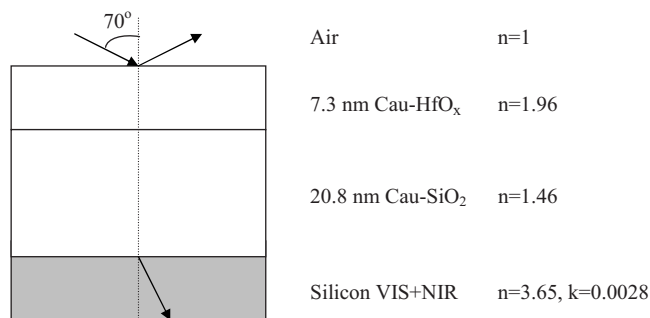
FIG. 4. Ellipsometric modeling and fit results of grown thin HfO$_2$ film.

ness of the SiO$_2$ film was also left variable as a fitting parameter since growing Si-oxide film at the interface between the grown HfO$_2$ film and Si substrate during dc sputtering at a 200 °C substrate temperature may also be possible. Other parameters of the fitting were the thickness and refractive index of the HfO$_2$ thin film. Then, the constructed model was fitted for the HfO$_2$ thin film using the Cauchy dispersion relation since HfO$_2$ is transparent in the spectral range of interest, i.e., $\lambda > 350$ nm. The equations for the Cauchy dispersion model are

$$n(\lambda) = n_0 + C_0 \frac{n_1}{\lambda^2} + C_1 \frac{n_2}{\lambda^4}, \qquad (3)$$

$$k(\lambda) = k_0 + C_0 \frac{k_1}{\lambda^2} + C_1 \frac{k_2}{\lambda^4}, \qquad (4)$$

where $C_0 = 10^2$ and $C_1 = 10^7$, λ is in nanometers, and n_0, n_1, n_2, k_0, k_1, and k_2 are numbers to be fitted with respect to wavelength.

The measured SE data, namely, Δ and Ψ, with the 70° incidence angle of light over the used spectral range, i.e., 300–850 nm, from the HfO$_2$ film on c-Si(100) with respect to wavelength and corresponding energy scale are shown in Fig. 5. It is also apparent from absorption and transmission versus wavelength plots that the grown HfO$_2$ film is transparent to the light in the range of $\lambda > 350$ nm (Fig. 6). As a result of the fit to the measured data by means of the Cauchy dispersion relation, the thickness of the hafnium-oxide medium is 7.3 nm while the refractive index is found to be 1.98 at 632 nm (Fig. 7). When compared to the thickness of the HfO$_2$ layer, however, a very thick SiO$_x$ interfacial layer, 20.8 nm, is formed between the Si substrate and the HfO$_2$ film.
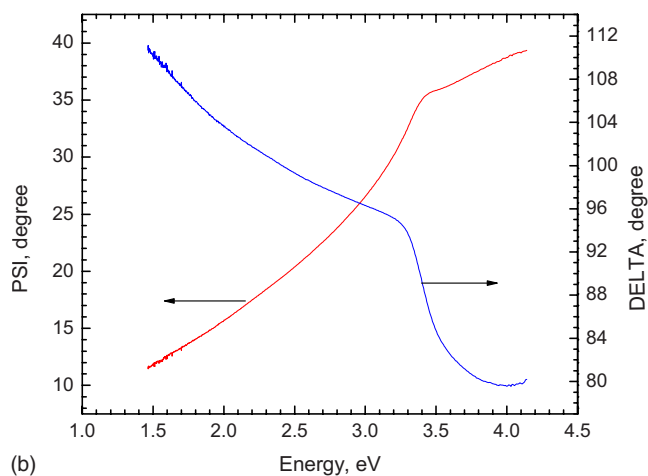
D. XPS spectroscopy

1. Si depth profile of the film

The XPS depth profile of the Si 2p signals of the reactively sputtered Hf-oxide film on the p-type (100) silicon substrate with native oxide is given in Figs. 8(a)–8(c). It is well known that the Si 2p spectra can be decomposed into five contributions: one is from the elemental Si (Si^0), three suboxides, i.e., Si$_2$O (Si^{1+}), SiO (Si^{2+}), and Si$_2$O$_3$ (Si^{3+}), and the native oxide SiO$_2$ (Si^{4+}).[23] The signals obtained at around 99.3 eV are the result of elemental (metallic) Si (Si^0), while the higher binding energies until around 104 eV correspond
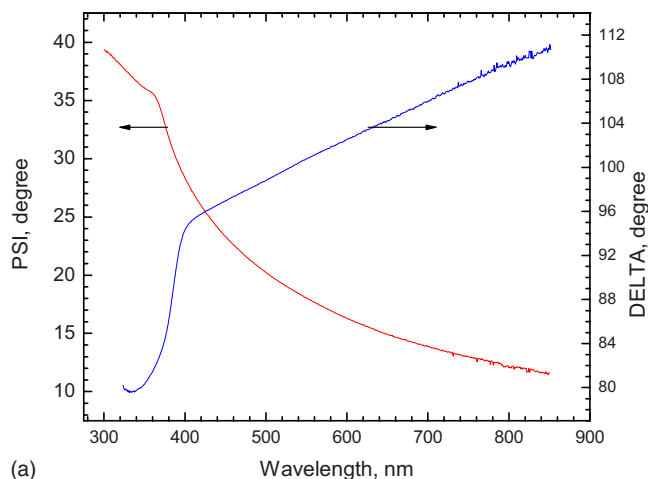
FIG. 5. (Color online) Spectroscopic ellipsometrically measured Ψ and Δ with respect to (a) wavelength and (b) photon energy.

to the oxidation states of Si; the lower binding energy ones (suboxides) are closer to the metallic Si, and the highest energy one corresponds to Si^{4+}.[24]

It is clearly seen in Fig. 8(b) that the elemental Si^0 is started to be seen at the very surface layers, i.e., starting from the fourth etching cycle and continuing until the depth of the oxide. It is clear that the intensity of elemental Si at these layers is at a very detectable level. However, its intensity through the depth of the oxide is decreased, but after some level of depth, it started to increase, gradually reaching the same intensity levels of the oxide form of Si, i.e., SiO$_x$ [Fig. 8(c)] and being the dominant mode in a few etching cycles, i.e., after the 12th cycle (Fig. 8(a)). Therefore, it can be inferred from the XPS depth profiling, as well as confirmed with the ellipsometric analysis, that there is a very broad interfacial oxide region since the substrate is reached after the 17th etching cycle with XPS.

Figure 8(c) shows the oxide form of the Si 2p signal. It corresponds to the native oxide form of Si at around 104 eV, namely, SiO$_2$ (Si^{4+}) close to the surface layer. However, the peak positions shift to lower energy levels ranging between 102.7 and 103 eV (~ 3.4–3.7 eV far from the region of the elemental Si signal) corresponding to the suboxide form of Si (SiO$_x$) and hafnium silicate (HfSi$_x$O$_y$) when the deeper layers are reached.[25–28]
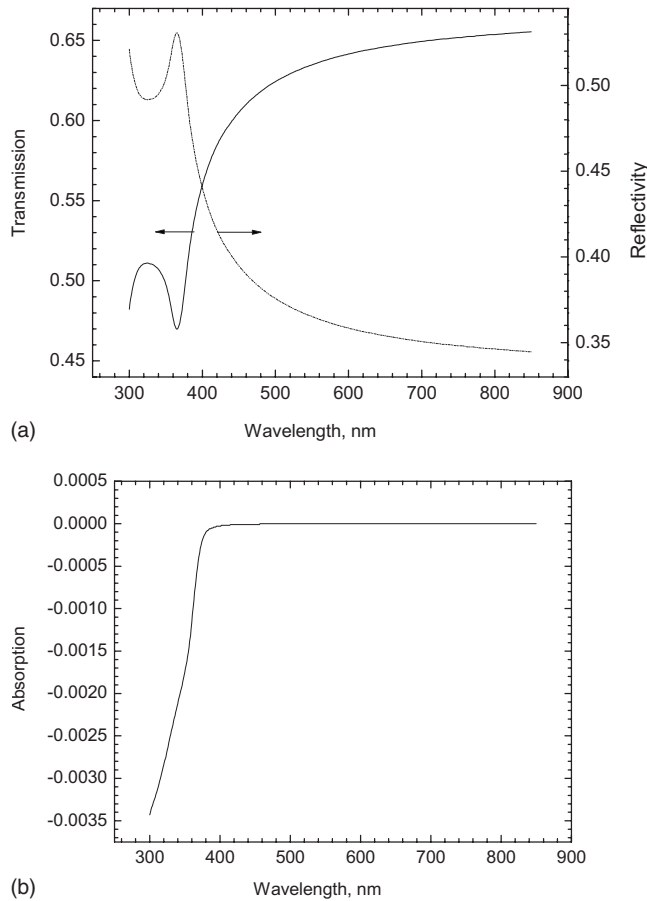
(a)

(b)

FIG. 6. (a) Transmission and reflectivity vs wavelength, (b) absorption vs wavelength.

The chemical shift for Si^{3+}, i.e., the difference in the binding energy of the component and that of elemental Si, is generally obtained at about 2.48–2.65 eV far from the position of elemental Si, i.e., 99.3 eV.[26] This chemical shift was, however, obtained $\sim$3.4–3.7 eV for deeper layers of the oxide. Since this shift is equal to that of neither Si^{4+} nor S^{3+}, and being very close to that of Si^{4+}, this can be inferred as the oxide containing Hf–O–Si, i.e., Hf silicate
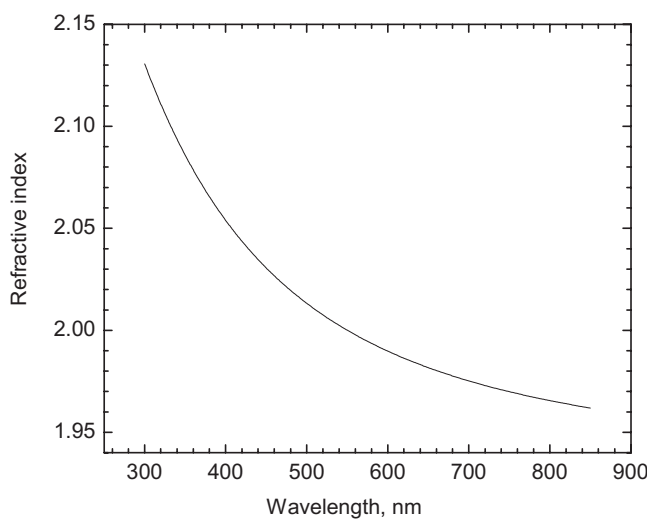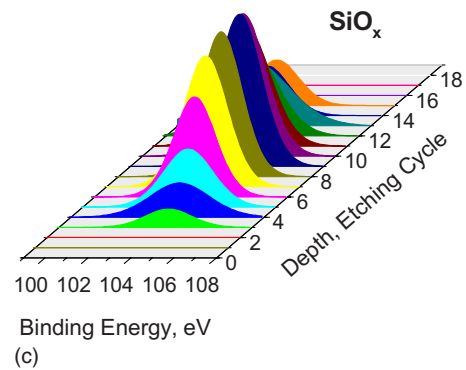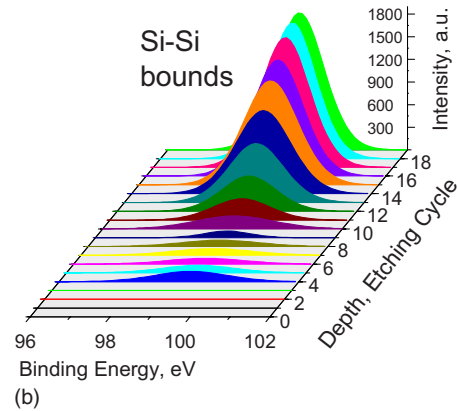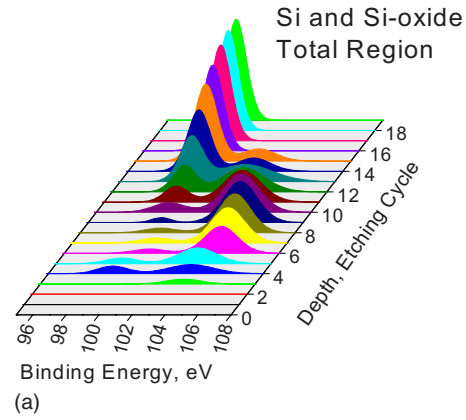

FIG. 7. Refractive index vs wavelength.

(a)

(b)

(c)

FIG. 8. (Color online) Si 2p spectra.

$(HfSi_xO_y)$.[26–28] The existence of this thick layer was also supported from the FTIR absorption spectrum (Fig. 2).

It was also realized by other research groups that highly active Hf atoms react with SiO_2 to obtain its oxygen, leaving either Si suboxide or elemental Si behind and forming Hf oxide instead.[6]

2. O 1s spectrum

Figure 9 shows the depth profile evolution of the O 1s spectrum. The lower energy state centered at about 530 eV for the very surface layer, i.e., zeroth to third cycle, is attributed to oxygen bonds in HfO_2.[7] The C peak exists only at the first layer. At deeper layers, the main peak is shifted to higher binding energy levels to $\sim$531.5 eV, which is explained as the detection of O bonds in nonstoichiometric $HfSi_xO_y$.[7,29] O 1s spectrum has a distinct peak located at $\sim$532.9 eV for SiO_2.[2] After the very surface layer, i.e., at the fourth and fifth etching cycles, the main peak is decomposed into two sub-
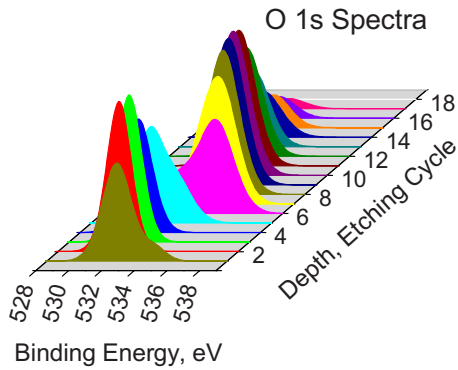
FIG. 9. (Color online) O 1s spectrum for depth profiling.

FIG. 11. (Color online) Quantification of constituting materials with respect to depth starting from the surface obtained from XPS depth profiling feature.

peaks, centered at about 531.5 and 533 eV corresponding to Hf silicates (HfSi$_x$O$_y$) and SiO$_x$. Simultaneously, the peaks are shifted to 533 eV corresponding to Si oxide until the 12th etching cycle. Then, there is a shift to lower binding energies corresponding to silicate formation, i.e., HfSi$_x$O$_y$, before the Si substrate is reached, i.e., from the 12th to the 17th etching cycles. The oxide after this etching level corresponds to the substrate and, therefore, does not contain oxygen.

3. Hf 4f peak

The depth profile of the Hf 4f spectrum is given in Fig. 10. We see in Fig. 10(a) that all levels containing hafnium oxide can be decomposed into two contributions. Fang *et al.*[7] showed that Hf 4f has a spin-orbit splitting of 1.6 eV at 16.90 and 18.50 eV for Hf 4$f_{7/2}$ and 4$f_{5/2}$, respectively, for HfO$_2$. However, these peaks shift to higher binding energies in the vicinity of Si, i.e., to 17–17.5 eV, for Hf 4$f_{7/2}$, which can be attributed to HfSi$_x$O$_y$.
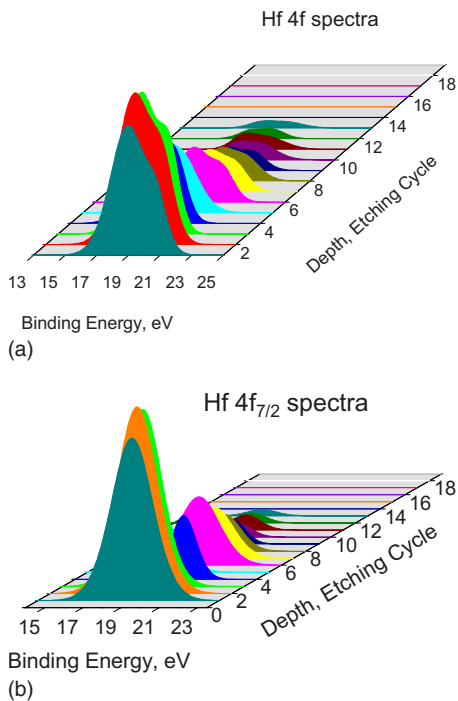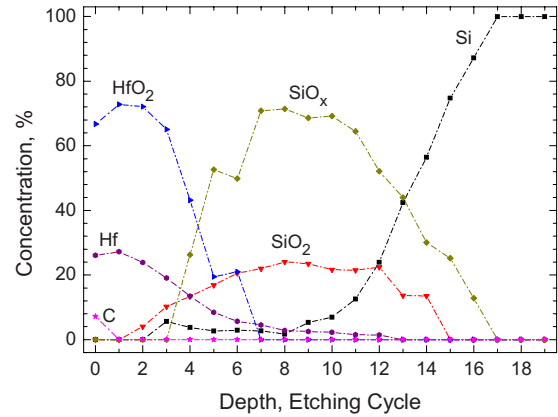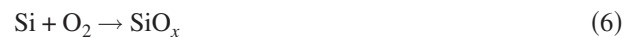

FIG. 10. (Color online) XPS depth profiling of Hf 4f spectrum for (a) Hf 4f spectra and (b) Hf 4f 7/2 spectra.

Figure 10 shows that the peaks for the first round of etching cycles belong to the HfO$_2$ mode; however, the peaks shift to the higher binding energy side when the sixth etching cycle was reached. Therefore, it is clear and also supported by the FTIR spectra (Fig. 2) that the HfSi$_x$O$_y$ mode is effective for a thick layer until the tenth cycle. Then, the peaks again start to be shown in the position of the HfO$_2$ mode and last until the substrate is reached. It is also clear from this figure that there is no indication of the presence of HfSi$_x$.

The XPS depth profiling analysis for quantification was performed on HfO$_2$/SiO$_2$/Si stacks, as shown in Fig. 11. The HfO$_2$ top layer is very thin compared to the interface layer constituted mainly from SiO$_x$ and SiO$_2$. The surface layer contains also carbon, i.e., C, as well as, Hf and O contributions. It can be seen from the figure that the areas calculated for the surface layer spectrum are given as 67% for O, 26% for Hf, and 7% for C. Therefore, the possible formation can be given as (26% Hf+52% O) for HfO$_2$, and the rest is (7% C+15% O) with CO$_{2.1}$.

It is clear that the broad interfacial layer is formed mainly from the 5th to the 12th etching cycle, and the substrate is reached at the 17th etching cycle. Elemental Si is detected at a level very close to the top layer, namely, third and fourth cycles even before the SiO$_2$ dominant layers. Then, its quantity gets diminished in the interfacial region even though it exists in small amounts almost all over the depth. This behavior of having a reasonable amount of elemental Si very close to the top layer of HfO$_2$ gives the idea of causing elementally active Hf radicals to decompose the native SiO$_2$ to form elemental Si explicitly and use the oxygen gained from these SiO$_2$ to form HfO$_2$. This process can be roughly given by the following chemical reactions:

$$Hf + SiO_2 \rightarrow HfO_2 + Si \tag{5}$$

$$Si + O_2 \rightarrow SiO_x \tag{6}$$

$$SiO_x + HfO_{x<2} + O_2 \rightarrow HfSi_xO_y \tag{7}$$

IV. CONCLUSION

A HfO$_2$/SiO$_2$/p-Si(100) stack was studied by means of FTIR, SE, XRD, and XPS depth profiling analyses. The re-

sults show that there is an extremely thin HfO_2 layer on top of a respectively broad interfacial layer formed mainly from Si suboxide and Hf silicate. Having elemental Si in the top layer and closer to the Hf-oxide layer side of the interfacial layer, it is concluded that Hf radicals consume the oxygen of native SiO_2 film to form Hf oxide by leaving elemental Si behind. This subsequent reactive deposition of HfO_2 on the native SiO_2/p-Si(100) stack leads to an interface with Si rich silicates with the very top thin HfO_2 layer.

It is clearly explained with the XPS depth spectra that the formation of $HfSi_x$ was eliminated since there is no direct contact of sputtered Hf with Si substrate. It was also shown that there exists a very thin perfect Hf-oxide layer, later Si–Si bonds are detected even before a Si suboxide layer is reached, and then Si substrate is reached. Since Si–Si bonds were measured just before Si oxide is reached, it can be realized that highly reactive sputtered Hf atoms consume some of the oxygen atoms from the underlying SiO_2 to form hafnium oxide by leaving Si–Si bonds behind, which supports what Yamamoto et al.[13] revealed with their experiment that the oxygen radicals oxidize the Hf metal more selectively than Si substrate. In this work, we showed, additionally, that Hf radicals even ionize SiO_2 to use its oxygen to form HfO_2, just leaving either elemental Si or Si suboxide behind.

The FTIR spectrum gives a result parallel to what was obtained with the XPS depth profile that there exists a very dominant and thick Si suboxide layer when compared to the extremely thin HfO_2 layer at the very surface of the grown film. This reality was also proved with the ellipsometric measurement of the grown film (Fig. 4). XRD measurement shows that the microcrystallinity has just started to form, having the (111) monoclinic phase of HfO_2, which is also supported by the FTIR absorption spectra.

ACKNOWLEDGMENTS

[1] G. D. Wilk, R. M. Wallace, and J. M. Anthony, J. Appl. Phys. **89**, 5243 (2001).
[2] P. D. Kirsch, C. S. Kang, J. Lozano, J. C. Lee, and J. G. Ekerdt, J. Appl. Phys. **91**, 4353 (2002).
[3] I. Barin, *Thermodynamical Data of Pure Substances* (VCH, Weinheim, 1989).
[4] S. Hayashi, K. Yamamoto, Y. Harada, R. Mitsuhashi, K. Eriguchi, M. Kubota, and M. Niwa, Appl. Surf. Sci. **216**, 228 (2003).
[5] R. Tan, Y. Azuma, and I. Kojima, Appl. Surf. Sci. **222**, 346 (2004).
[6] R. Tan, Y. Azuma, and I. Kojima, Surf. Interface Anal. **38**, 784 (2006).
[7] Q. Fang, J.-Y. Zhang, Z. Wang, M. Modreanu, B. J. O'Sullivan, P. K. Hurley, T. L. Leedham, D. Hywel, M. A. Audier, C. Jimenez, J.-P. Senateur, and I. W. Boyd, Thin Solid Films **453–454**, 203 (2004).
[8] R. Thielsch, A. Gatto, J. Heber, and N. Kraiser, Thin Solid Films **410**, 86 (2002).
[9] A. Deshpande, R. Inman, G. Jursich, and C. Takoudis, Microelectron. Eng. **83**, 547 (2006).
[10] J. Kim, S. Kim, H. Kang, J. Choi, H. Jeon, M. Cho, K. Chung, S. Back, K. Yoo, and C. Bae, J. Appl. Phys. **98**, 094504 (2005).
[11] J. Zhu, Z. G. Liu, and Y. Feng, J. Phys. D: Appl. Phys. **36**, 3051 (2003).
[12] G. Aygun and R. Turan, Thin Solid Films **517**, 994 (2008).
[13] K. Yamamoto, S. Hayashi, M. Niwa, M. Asai, S. Horii, and H. Miya, Appl. Phys. Lett. **83**, 2229 (2003).
[14] G. He, L. D. Zhang, and Q. Fang, J. Appl. Phys. **100**, 083517 (2006).
[15] T. C. Chen, C. Y. Peng, C. H. Tseng, M. H. Liao, M. H. Chen, C. I. Wu, M. Y. Chern, P. J. Tzeng, and C. W. Liu, IEEE Trans. Electron Devices **54**, 759 (2007).
[16] D. A. Neumayer and E. Cartier, J. Appl. Phys. **90**, 1801 (2001).
[17] E. Atanassova, G. Aygun, R. Turan, and Tz. Babeva, J. Vac. Sci. Technol. A **24**, 206 (2006).
[18] L. Pereira, A. Marques, H. Aguas, N. Nedev, S. Georgiev, E. Fortunato, and R. Martins, Mater. Sci. Eng., B **109**, 89 (2004).
[19] S. W. Nam, J. H. Yoo, S. Nam, H. J. Choi, D. Lee, D. H. Ko, J. H. Moon, J. H. Ku, and S. Choi, J. Non-Cryst. Solids **303**, 139 (2002).
[20] G. He, M. Liu, L. Q. Zhu, M. Chang, Q. Fang, and L. D. Zhang, Surf. Sci. **576**, 67 (2005).
[21] H. G. Tompkins and W. A. McGahan, *Spectroscopic Ellipsometry and Reflectometry* (Wiley, New York, 1999).
[22] I. I. Suni, J. Appl. Electrochem. **27**, 1219 (1997).
[23] S. Yerci, I. Yildiz, M. Kulakci, U. Serincan, M. Barozzi, M. Bersani, and R. Turan, J. Appl. Phys. **102**, 024309 (2007).
[24] G. Aygun, E. Atanassova, K. Kostov, and R. Turan, J. Non-Cryst. Solids **352**, 3134 (2006).
[25] G. He, L. D. Zhang, G. W. Meng, G. H. Li, G. T. Fei, X. J. Wang, J. P. Zhang, M. Liu, Q. Fang, and I. W. Boyd, J. Appl. Phys. **104**, 104116 (2008).
[26] J. Maunoury, K. Dabertrand, E. Martinez, M. Saadoune, D. Lafond, F. Pierre, O. Renault, S. Lhostis, P. Bailey, T. C. Q. Noakes, and D. Jalabert, J. Appl. Phys. **101**, 034112 (2007).
[27] O. Renault, D. Samour, J. F. Damlencourt, D. Blin, F. Martin, S. Marthon, N. T. Barrett, and P. Besson, Appl. Phys. Lett. **81**, 3627 (2002).
[28] N. Barrett, O. Renault, J. F. Damlencourt, and F. Martin, J. Appl. Phys. **96**, 6362 (2004).
[29] G. D. Wilk, R. M. Wallace, and J. M. Anthony, J. Appl. Phys. **87**, 484 (2000).